Int Journ Earth Sciences (1999) 88:60–75

ORIGINAL PAPER

J. Peckmann · V. Thiel · W. Michaelis · P. Clari
C. Gaillard · L. Martire · J. Reitner

Cold seep deposits of Beauvoisin (Oxfordian; southeastern France) and Marmorito (Miocene; northern Italy): microbially induced authigenic carbonates

Received: 13 October 1998 / Accepted: 5 February 1999

Abstract The relation of two well-known ancient carbonate deposits to hydrocarbon seepage was confirmed by this study. Archaea are found to be associated with the formation of Oxfordian seep carbonates from Beauvoisin and with a Miocene limestone from Marmorito ("tube-worm limestone"). Carbonates formed due to a mediation by archaea exhibit extremely positive or extremely negative $\delta^{13}C_{carbonate}$ values, respectively. Highly positive values (+15‰) reflect the use of ^{13}C-enriched CO_2 produced by methanogenesis. Low $\delta^{13}C$ values of the Marmorito carbonates (–30‰) indicate the oxidation of seepage-derived hydrocarbons. Likewise, the $\delta^{13}C$ content of specific tail-to-tail linked isoprenoids, biomarkers for archaea, was found to be strikingly depleted in these samples (as low as –115‰). The isotopic signatures corroborate that archaea were involved in the cycling of seepage-derived organic carbon at the ancient localities. Another Miocene limestone ("Marmorito limestone") shows a strong imprint of methanotrophic bacteria as indicated by $\delta^{13}C$ values of carbonate as low as –40‰ and biomarker evidence. Epifluorescence microscopy and field-emission scanning electron microscopy revealed that bacterial biofilms were involved in carbonate aggregation. In addition to lucinid bivalves previously reported from both localities, we infer that sponges from Beauvoisin and tube worms from Marmorito depended on chemosynthesis as well. Low $\delta^{13}C$ values of nodules related to sponge taphonomy (–27‰) indicate that sponges might have been linked to an enhanced hydrocarbon oxidation. Tube worm fossils from Marmorito closely resemble chemosynthetic pogonophoran tube worms from Recent cold seeps and are embedded in isotopically light carbonate ($\delta^{13}C$ –30‰).

Key words Carbonates · Cold seeps · Methane · Petroleum · Archaea · Bacteria · Sponges · Tube worms · Epifluorescence · Biomarkers · Jurassic · Tertiary · France · Italy

J. Peckmann (✉) · J. Reitner
Institut und Museum für Geologie und Paläontologie, Georg-August-Universität, Goldschmidtstrasse 3, D-37077 Göttingen, Germany
e-mail: jpeckma@gwdg.de,
Fax: +49-551-397918

V. Thiel, W. Michaelis
Institut für Biogeochemie und Meereschemie, Universität Hamburg, Bundesstrasse 55, D-20146 Hamburg, Germany

P. Clari, L. Martire
Dipartimento di Scienze della Terra, via Accademia delle Scienze 5, I-10123 Torino, Italy

C. Gaillard
UFR des Sciences de la Terre, UMR 5565 Centre de Paléontologie stratigraphique et Paléoécologie, Université Claude Bernard, Lyon 1, 27–43 Boulevard du 11 Novembre, F-69622 Villeurbanne Cedex, France

Introduction

Recent and ancient cold seep carbonates

Seep carbonates are well-known products of the microbial oxidation of methane and other reduced gases seeping out from the sea floor. Since the past decade they have been documented from Recent and ancient seeps and vents situated in different geological settings. It has been suggested that sulphate reduction coupled with anaerobic oxidation of methane resulting in an increase in alkalinity is the driving reaction for the precipitation of carbonate at these sites (Ritger et al. 1987; Jörgensen 1989; Suess and Whiticar 1989). This hypothesis is supported by the abundance of pyrite in carbonates.

Mg-calcite, aragonite and dolomite are the common authigenic minerals at cold seeps (Roberts et al. 1993). In addition to micritic matrices, different types of carbonate-cements have been reported, such as

Reitz E (1992) Silurische Mikrosporen aus einem Biotit-Glimmerschiefer bei Rittsteig, Nördlicher Bayerischer Wald. N Jahrb Geol Paläontol Mh: 351–358

Reitz E, Höll R (1988) Jungproterozoische Mikrofossilien aus der Habachformation in den mittleren Hohen Tauern und dem nordostbayerischen Grundgebirge. Jahrb Geol BA 131:329–340

Röhr C (1990) Die Genese der Leptinite und Paragneise zwischen Nordrach und Gengenbach im mittleren Schwarzwald. Frankfurter Geowiss Arb Serie C 11:1–159

Sutherland SJE (1994) Ludlow chitinozoans from the type area and adjacent regions. Palaeontograph Soc Monogr Lond 148:1–104

Tait JA, Bachtadse V, Franke W, Soffel HC (1997) Geodynamic evolution of the European Variscan fold belt: palaeomagnetic and geological constraints. Geol Rundsch 86:585–598

Todt W (1976) Zirkon-U/Pb-Alter des Malsburg-Granits vom Südschwarzwald. N Jahrb Mineral Mh: 532–544

Todt WA, Büsch W (1981) U–Pb investigations on zircons from pre-Variscan gneisses. I. A study from the Schwarzwald, West Germany. Geochim Cosmochim Acta 45:1789–1801

Torsvik TH, Smethurst MA, Meert JG, Voo RVd, McKerrow WS, Brasier MD, Sturt BA, Walderhaug HJ (1996) Continental break-up and collision in the Neoproterozoic and Paleozoic: a tale of Baltica and Laurentia. Earth Sci Rev 40:229–258

Traverse A (1988) Paleopalynology. Unwin Hyman, Boston, pp 1–600

Vogler WS (1995) Who can survive high-pressure metamorphism? Bochumer Geol Geotech Arb 44:250–254

Wada H, Tomita T, Matsuura K, Iuchi K, Ito M, Morikiyo T (1994) Graphitization of carbonaceous matter during metamorphism with reference to carbonate and pelitic rocks of contact and regional metamorphisms, Japan. Contrib Mineral Petrol 118:217–228

Wang G-F (1989) Carbonaceous material in the Ryoke metamorphic rocks, Kinki district, Japan. Lithos 22:305–316

Wendt JI, Kröner A, Fiala J, Todt W (1993) Evidence from zircon dating for existence of approximately 2.1 Ga old crystalline basement in southern Bohemia, Czech Republic. Geol Rundsch 82:42–50

Wickert F, Altherr R, Deutsch M (1990) Polyphase Variscan tectonics and metamorphism along a segment of the Saxothuringian–Moldanubian boundary: the Baden-Baden Zone, northern Schwarzwald (F.R.G.). Geol Rundsch 79:627–647

Wimmenauer W (1988) Precambrian in the horst mountains of the Rhine graben area. In: Zoubek V (ed) Precambrian in younger fold belts. European Variscides, the Carpathians and Balkans. Wiley, Chichester, pp 381–408

Wopenka B, Pasteris JD (1993) Structural characterization of kerogens to granulite-facies graphite: applicability of Raman microprobe spectroscopy. Am Mineral 78:533–557

Zulauf G, Dörr W, Fiala J, Vejnar Z (1997) Late Cadomian crustal tilting and Cambrian transtension in the Teplá-Barrandian unit (Bohemian Massif, Central European Variscides). Geol Rundsch 86:571–584

Table 1. Compilation of types of cold seep carbonates analysed in this study and their characteristics

Cold seep carbonate	Frequent fossils	Carbonate species	Stable isotopes	Biomarkers
Beauvoisin				
Lower Oxfordian carbonates	Lucinid bivalves Sponges Gastropods Cephalopods Crustaceans Foraminifera Ostracods	Mg-calcite Calcite Dolomite Aragonite	$\delta^{13}C$: –26.5 to +13.0‰ $\delta^{18}O$: –7.1 to +2.9‰	*n*-alkanes
Middle and Upper Oxfordian carbonates	See Lower Oxfordian carbonates, sea urchin	Calcite	$\delta^{13}C$: –13.6 to +15.1‰ $\delta^{18}O$: –1.2 to +0.7‰	*n*-alkanes PME Squalane
Marmorito				
Lucina limestone	Lucinid bivalves Foraminifera	Calcite	$\delta^{13}C$: –35.5 to -0.1‰ $d^{18}O$: +0.1 to +4.9‰ (Clari et al. 1994)	Not analysed
Tube-worm limestone	Tube worms Foraminifera	Calcite	$\delta^{13}C$: -32.9 to -26.6‰ $\delta^{18}O$: -0.4 to +0.1‰	Crocetane PME
Botryoidal aragonite	None	Aragonite	$\delta^{13}C$: -34.8 to -27.0‰ $\delta^{18}O$: +0.3 to +2.7‰	Not analysed
Marmorito limestone	None	Dolomite Calcite	$\delta^{13}C$: -40.2 to –17.3‰ $\delta^{18}O$: +4.8 to +4.9‰	Methyl-sterols Methyl-hopanols

botryoidal aragonite or calcite, splayed calcite and yellow calcite (Beauchamp and Savard 1992). It has been presumed that botryoids are of bacterial origin (Roberts et al. 1993).

Negative $\delta^{13}C$ values of seep carbonates are related to the microbial oxidation of thermogenic (–50‰ PDB) and biogenic (–60 to –110‰ PDB) methane (Whiticar et al. 1986; Hovland et al. 1987). The lowest $\delta^{13}C$ values measured for carbonates from Recent cold vents are –53.9‰ PDB (Roberts et al. 1993), –56.1‰ PDB (Hovland 1987) and –66.7‰ PDB (Ritger et al. 1987).

The macro-fauna associated with cold vents is dominated by mussels, clam bivalves and tube worms (Paull et al. 1984; Kennicutt et al. 1985; Suess et al. 1985; Juniper and Sibuet 1987; Rosman et al. 1987; Hashimoto et al. 1989; Callender et al. 1990). These invertebrates harbour chemolithotrophic or methanotrophic bacteria which supply their hosts with energy and nutrients by oxidizing reduced sulfur species or methane (Jannasch 1984).

The interpretations of fossil seep sites are based on features similar to their modern counterparts, i.e. negative $\delta^{13}C_{carbonate}$ values and the localized occurrence of particular macroinvertebrate taxa ("fossil seep-search strategy"; Campbell et al. 1993). Here we report on two well-known examples of fossil seep carbonates. Special emphasis is placed on microbially induced precipitation and on the relevance of taphonomic processes such as the bacterial degradation of soft tissues on the creation of bacterioform fabrics. Carbonate phases exhibiting enhanced concentrations of organic compounds were detected by epifluorescence microscopy. Furthermore, we applied organic geochemical techniques to trace molecular fingerprints of fossil chemosynthetic microbiota associated with the formation of these ancient rocks.

Beauvoisin

Beauvoisin is located in southeastern France near Buis-les-Baronnies (Drôme; Fig. 1). Cold seep carbonates are exposed within the thick succession of Jurassic black shales of the "Terres Noires" Formation in Lower Oxfordian to Upper Oxfordian strata (Gaillard et al. 1985). The fossiliferous carbonates have been characterized as pseudobioherms since they exhibit a bioherm-like shape but neither include reef-building organisms nor form a significant sea-floor relief. The pseudobioherms are situated along major faults that were probably active during the deposition of the "Terres Noires" Formation (Gaillard et al. 1985).

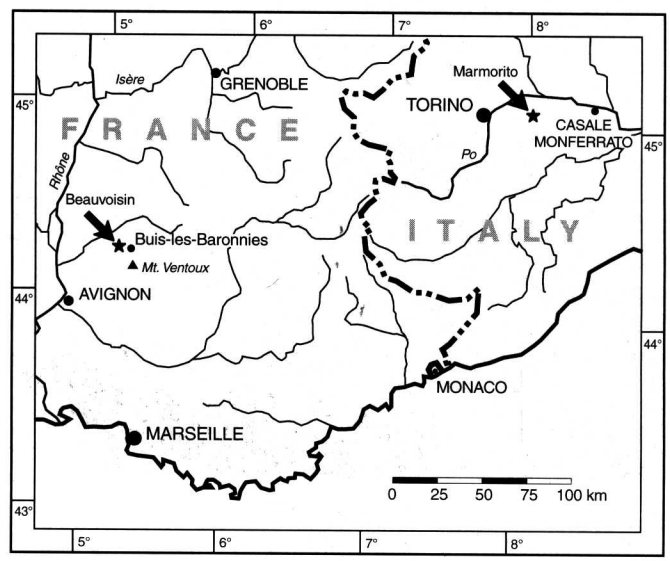

Fig. 1 Location of the Beauvoisin and Marmorito outcrops

Faulting occurred in an extensional tectonic regime along the continental margins due to the opening of the Tethyan Ocean during the late Jurassic (Gaillard et al. 1992). The pseudobioherms have a high carbonate content compared with the surrounding hemipelagites (85 vs 35% $CaCO_3$) and grew within the sediment near to the sediment–water interface.

Lower Oxfordian pseudobioherms are exposed in the dark, well-stratified marls of the upper part of the "Terres Noires" Formation (Fig. 2). They are large conical or lenticular carbonate buildups 1–10 m in height. Pseudobioherms contain a rich endofauna. Dominant organisms are endobenthic, large-sized bivalves (lucinids) which locally form very dense clusters similar to recent examples (cf. Sibuet and Olu 1998). Their palaeoecology has been studied and their communities have been found to be similar to those of recent hydrothermal vents and cold seeps (Rolin et al. 1990; Gaillard et al. 1992).

Middle and Upper Oxfordian pseudobioherms occur in the first limestone/marl alternations just above the "Terres Noires" Formation. Most of them are exposed in the basal "Argovian sequence" which corresponds to the Transversarium zone. The pseudobioherms form small lenses or columns of 1–2 m in height and width (Fig. 3). They laterally pass into beds which can be distinguished throughout the whole southeastern France basin (Gaillard et al. 1992). A genetic relation between these pseudobioherms and synsedimentary tectonics has been demonstrated by Gaillard and Rolin (1988).

Marmorito

Cold seep deposits occur near the village of Marmorito in the Monferrato hills, east of Torino in northern Italy (Fig. 1). The seep carbonates are embedded in the Miocene strata of the western Monferrato hills, most of which consist of coarse- to fine-grained siliciclastic sediments deposited in a slope to inner shelf environment (Clari et al. 1988). The sequence of the Tertiary Piedmont Basin is considered to be posttectonic, as the

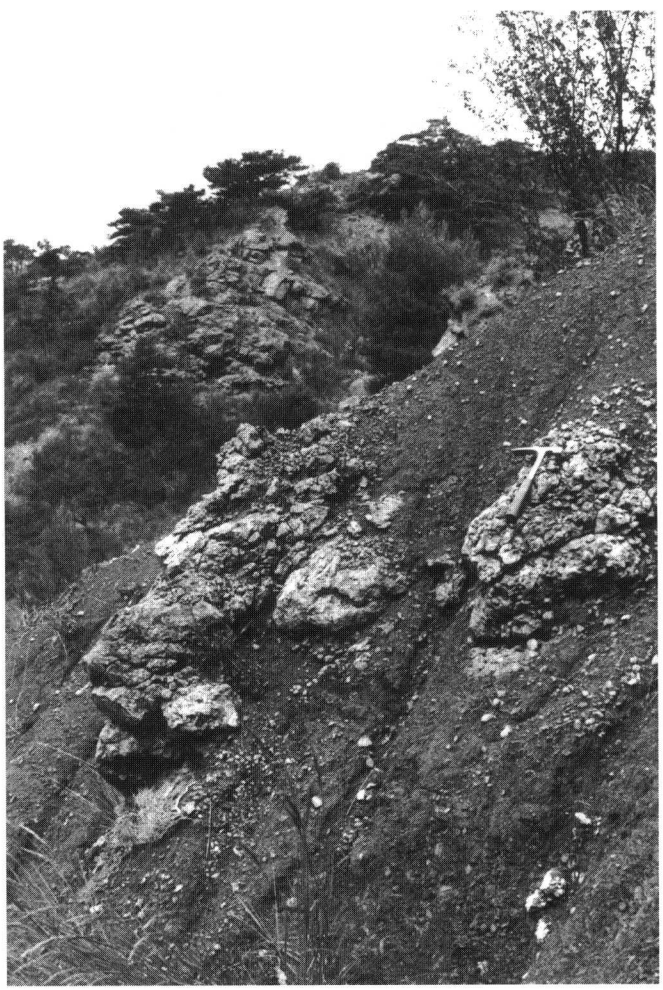

Fig. 2 Two Lower Oxfordian pseudobioherms (fore- and background) embedded in dark marlstones of the Terres Noires Formation. The *pseudobioherm in the background* is approximately 10 m in height and 15 m in width, Beauvoisin

Fig. 3 Middle Oxfordian pseudobioherm, Beauvoisin

weak superimposed Tortonian to early Pliocene lateral thrusting of the Monferrato hills vanishes towards the Collina di Torino structure in the west (Ricci Lucchi and Vai 1994). Marmorito is one of the first examples for which a relationship of ancient methane venting, fossil chemosynthetic bivalve communities, and methane-related carbonate precipitation has been demonstrated (Clari et al. 1988, 1994). The interpretation was based on the isotopic composition of carbonates ($\delta^{13}C$ values as low as –35‰) and on the presence of bivalve assemblages similar to those of modern seeps. Clari et al. (1988) reported two different types of methane-related carbonates, the *Lucina* limestone and the Marmorito limestone.

The *Lucina* limestone is a light-brown marly limestone, packed with bivalve (lucinid) molds. Its mineralogy is calcitic. The micro-crystalline, extremely hard Marmorito limestone appears to be barren of fossils and exhibits either a calcitic or dolomitic mineralogy. A typical feature of the Marmorito limestone is a chaotic fabric due to an intense brecciation.

Methods

Standard petrographic microscopy was performed on thin sections (150×100, 100×75 and 48×28 mm). For petrographical staining a mixture of potassium ferricyanide and alizarin red, dissolved in 0.1% HCl, was used. Aragonite was stained with Feigl's solution (Feigl 1958). Titan-Yellow staining allowed the estimation of the Mg content of calcite (Choquette and Trusell 1978) by comparison with stained calcites of known Mg content. Mg measurements were performed with atomic absorption spectrometry on a Philips PU 9200X (Philips, Best, The Netherlands). Fluorescence microscopy was carried out on a Zeiss Axiolab (lamp: HBO 50; filters: BP 365 FT 395 LP 397 and BP 450–490 FT 510 LP 520). A Leo 1530 Gemini was used for field-emission scanning electron microscopy on uncoated samples that were etched with 1% HCl for 1 min. Samples for oxygen and carbon stable isotopic analyses were taken from the surfaces of polished blocks using a handheld microdrill. Carbon dioxide for analyses was obtained by reacting the sample with 100% orthophosphoric acid in vacuo at 25 °C, and was analysed in a Finnigan MAT 251. The $\delta^{13}C$ and $\delta^{18}O$ results are reported relative to the PDB standard (SD < 0.04%) and appropriate correction factors were applied (Craig 1957). A correction factor for $\delta^{18}O$ values of –0.57‰ (Kim and O'Neil 1997) was added to the aragonite samples and a correction factor of –0.8‰ (Sharma and Clayton 1965) was added to the $\delta^{18}O$ values of dolomite samples. X-ray diffraction (XRD) was carried out on unoriented slurries using a diffractometer with Cu Ka radiation (Philips PW 1800, Philips, Best, The Netherlands). For biomarker analyses the carbonates were carefully cleaned (diluted HCl, acetone) and decalcified (diluted HCl). The residues were washed to a pH of >5, and dried. After saponification (6% KOH in CH_3OH), the supernatant was decanted and the residue further extracted three times with CH_2Cl_2/CH_3OH (3:1 v:v, ultrasonication 3×20 min). Subsequently, the combined supernatants were extracted with CH_2Cl_2 vs water (pH2). The organic substances of the CH_2Cl_2 phase were fractionated by column chromatography (Merck silica gel 60). Hydrocarbons were eluted with *n*-hexane, and an alcohol/ester fraction with CH_2Cl_2. Prior to further analyses, alcohols were converted to acetates by treatment with pyridine/acetic acid anhydride (1:1; v:v). All analyses were run on a Carlo Erba Fractovap 4160 gas chromatograph (GC) using a 30 m fused silica capillary column (DB5, 0.32 mm i.d., 0.25-μm film thickness), on-column injection and a flame ionization detector. Compound identifications were based on coupled gas chromatography/mass spectrometry (GC-MS). The GC-MS system used was a Finnigan MAT CH7A mass spectrometer interfaced to a Carlo Erba 4160 gas chromatograph, equipped with a 50-m fused silica capillary column (DB5HT, 0.3 mm i.d., 0.25 μm film thickness) and on-column injection. Helium was used as carrier gas. Compound-specific isotopic signatures were analysed by GC-combustion-isotope ratio mass spectrometry (GC-C-IRMS) and were performed on a Finnigan MAT 252 mass spectrometer controlled by Isodat software. Isotope ratios are reported as δ-values [$\delta^{13}C$ (‰), relative to the PDB standard]. The measurements were calibrated against internal standards of known isotopic composition (s = < 1‰).

Results

Seep biota

Beauvoisin

Mollusks are the most frequent macro-fossils in Lower Oxfordian carbonates (see Table 1). They are dominated by large lucinid bivalves which are confined to pseudobioherms where they may form dense clusters (Fig. 4a). The largest specimens reach 18 cm in length. When preserved, the outer layer of the shell provides positive $\delta^{13}C$ values as high as +5‰. These values are probably related to the symbiotic community with chemosynthetic bacteria (Rolin et al. 1990; Gaillard et al. 1992). Other mollusks include various gastropods and cephalopods (mainly ammonites) which probably thrived on the rich food supply provided by bivalves and bacteria. Crustacean exoskeletons, fragments and coprolites, as well as fish teeth, reflect the presence of additional predators or scavengers. The crustacean coprolites belong to the form-genus *Favreina* (Brönnimann 1955), which is attributed to the anomuran superfamilies Thalassinoidea and Galatheoidea (Brönnimann 1972). Probable deposit feeders, such as holothuroids (sclerites), and suspension feeders, such as

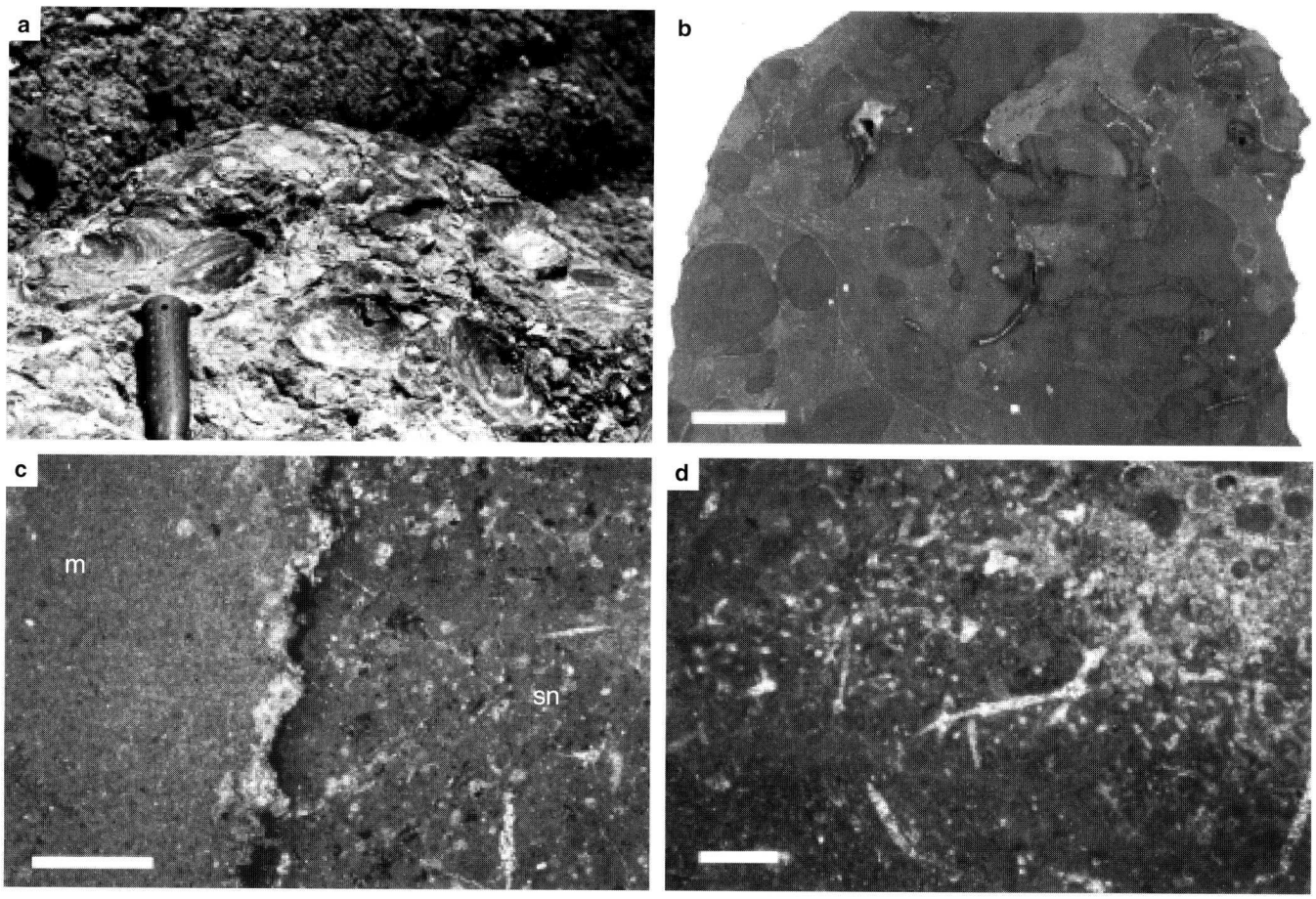

Fig. 4a–d Lower Oxfordian carbonates and associated biota, Beauvoisin. **a** Massive limestone with lucinid bivalves. **b** Polished slab showing the typical nodular fabric of the seep carbonates. The *scale bar* corresponds to 1.5 cm. **c** Sponge nodule (*sn*) lined by an outer rim of pyrite and within the micro-crystalline matrix (*m*). The *scale bar* corresponds to 1 mm. **d** Sponge nodule with hexactinellid spicules and the typical clotted, bacterioform fabric. The *scale bar* corresponds to 100 μm

crinoids (ossicles), are found in minor abundance. These biota are common in bathyal environments of the Jurassic sea floor and are not restricted to vents. Among the microfauna benthic foraminifers (Spirillinidae, Nodosariidae, Textulariidae, *Ophthalmidium*) and ostracods predominate. Planktonic foraminifers (Globigerinidae), radiolarians and dinoflagellates are present but less numerous.

Sponges are also frequent within Lower Oxfordian carbonates. Lyssacid hexactinellids are most common and are accompanied by "lithistid" demosponges, unidentified demosponges and lychniscid hexactinellids. Some fossilized sponge bodies were found, but nodular aggregates containing spicules are much more common. These nodules are darker than the micritic matrix, in which they are embedded. They contain framboidal pyrite and are often lined by an outer rim of pyrite (Fig. 4c). Internally the nodules exhibit a clotted fabric (Fig. 4d).

Abundance of fossils is low in Middle and Upper Oxfordian limestones. Apart from that the fauna is very similar to the Lower Oxfordian carbonates. A remarkable feature of some pseudobioherms is the local mass occurrence of a small irregular sea-urchin *Tithonia* (Gaillard et al. 1992).

Marmorito

In contrast to the Marmorito limestone, the *Lucina* limestone contains a diverse fauna (see Table 1). The limestone is named after large, articulated clams found in this rock. Due to the preservation as molds, a taxonomic evaluation is not possible. Associated with the molds are peloids of two size classes. The diameter of the larger ones is approximately 1400×1000 μm but may reach 3000 μm. The smaller-sized peloids are approximately 140×110 μm in diameter. The microfacies of the *Lucina* limestone is dominated by planktonic foraminifers. Foraminifers may be so frequent that the rock can be termed a foraminiferal packstone. In rocks where they are most abundant clams recede. Planktonic foraminifers belong to the order *Rotaliida* with the genera *Globigerina* and *Orbulina* predominating. Benthic foraminifers and fragments of echinoids are also common.

A block of limestone with the remains of tube worms was found among blocks of the Lucina lime-

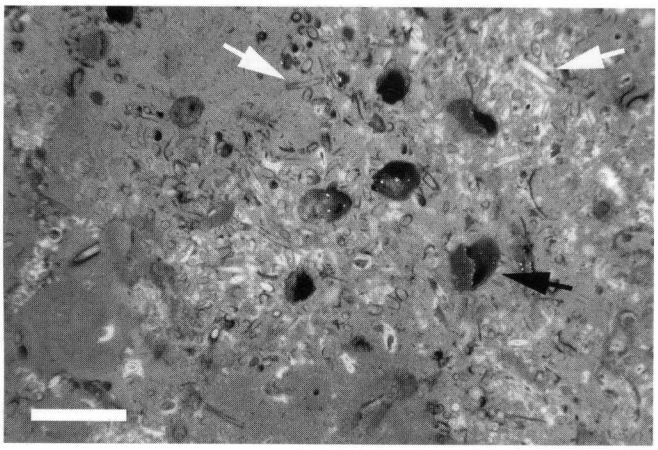

Fig. 5 Polished slab of the tube-worm limestone. The *white arrows* point to worm tubes and the *black arrow* points to a *Planolites-type* burrow, Marmorito. The *scale bar* corresponds to 1 cm

stone (Fig. 5). Tubes are arranged in dense clusters, predominantly in life position. The skeletons of tube worms were dissolved and resulting porosity is partly filled by calcitic cements. The interior of the tubes is filled with sediment and the diameter of molds varies from 700 to 1000 μm. The clusters are enclosed in a micritic, brownish-yellow sediment. The microfacies of the limestone with tube worms is similar to the *Lucina* limestone, but planktonic foraminifers are less frequent. *Planolites*-type burrows up to 5 mm in diameter cross the sediment (Fig. 5). The cylindrical burrows filled with micrite are curved and do not branch.

Seep carbonates

Beauvoisin

The Oxfordian seep carbonates are formed of micritic nodules. Nodules are densely packed in the centres and become scattered towards the margins, thus indicating a radial growth direction. Concretions formed around body fossils, such as ammonites and bivalves, are common. Other concretions are related to sponge taphonomy and burrowing (Fig. 4b). All kinds of nodules in the pseudobioherms are surrounded by fossiliferous micrites. Nodules and fossiliferous micrites consist of mainly non-ferroan, Mg-rich calcite. An intense red colour observed after Titan-Yellow staining is caused by a content of approximately 5 mole% $MgCO_3$. The limestones are locally recrystallized, forming a pseudospar with calcite crystals up to 25 μm in diameter. Bitumen is frequent and enriched in joints. Pyrite is rare in the fossiliferous matrix micrites but is common in the nodules related to sponge taphonomy. Framboids are arranged in clusters which range from 40 to 250 μm in diameter.

Joints caused by brecciation are filled by several generations of carbonate cements. The first generation is an iron-rich calcite of 20- to 300-μm-sized sub- to euhedral crystals. It may be followed by bladed, high-Mg-calcite or aragonite, but never by both phases in one section. The most remarkable cements are botryoidal aragonites up to 550 μm in radius which form the final cement generation. The botryoids originate on iron-rich calcite and grow into the free joint space (Fig. 6). Most botryoids are preserved in their original aragonitic mineralogy. Only a small portion become calcitized or micritized with the micritization directed from the centre to the periphery.

Dolomite makes up a significant portion of the rock volume. It occurs as partly ferruginous, euhedral rhomb-shaped crystals of approximately 100–140 μm in size, embedded in a micritic matrix. Dolomitization is very selective, affecting preferentially the inter-nodular micrites.

The Lower Oxfordian carbonates exhibit an intense fluorescence. The brightest fluorescence (yellow to white) is observed on the edges of micro-cavities and veins (Fig. 7). The micrites of the nodules exhibit a moderate brownish fluorescence which corresponds to the amount of framboidal pyrite. In neomorphic zones two phenomena are observed: (a) nodules appear when excited by ultraviolet light; and (b) pseudospars occasionally show a laminated fabric (Fig. 8).

The Middle and Upper Oxfordian limestones are made of homogeneous micrite. Framboidal pyrite is less common than in Lower and Middle Oxfordian carbonates. Calcitic cement is restricted to the interior of tubular cavities.

Marmorito

Lucina limestone and tube worm limestone. The molds of lucinid bivalves are enclosed in a packstone- or

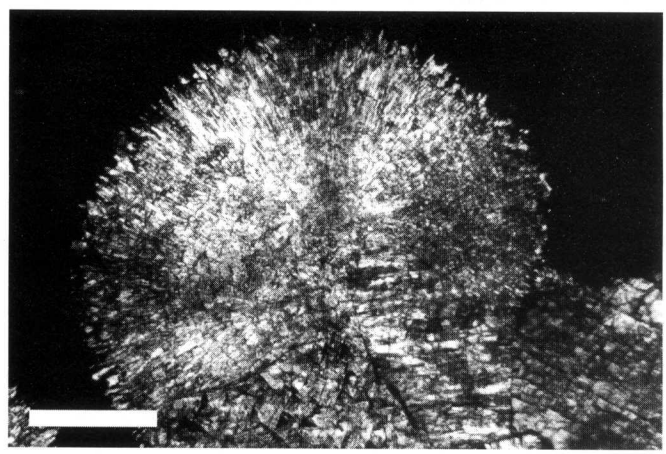

Fig. 6 Botryoidal aragonite originating on iron-rich calcite (XPL). Lower Oxfordian carbonate, Beauvoisin. The *scale bar* corresponds to 250 μm

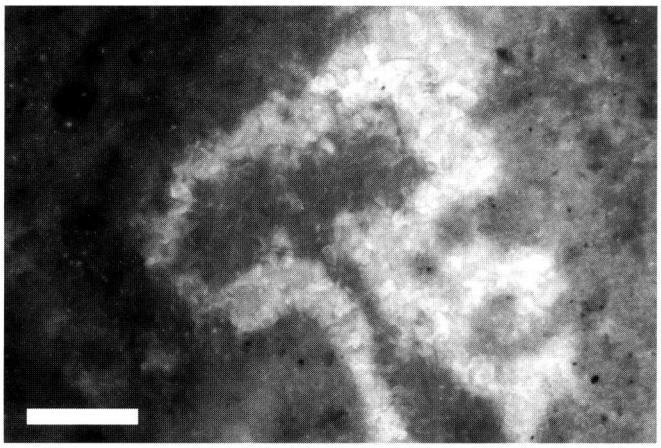

Fig. 7 Epifluorescence micrograph of a former micro-cavity which is now filled by calcite spar. Note the intense fluorescence on the edge of the cavity. Lower Oxfordian carbonate, Beauvoisin. The *scale bar* corresponds to 250 μm

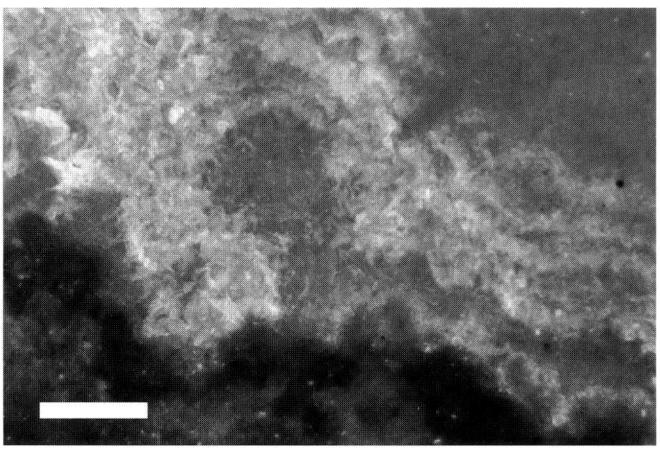

Fig. 8 Epifluorescence micrograph of a neomorphic zone which shows a laminated fabric due to excitation. Lower Oxfordian carbonate, Beauvoisin. The *scale bar* corresponds to 200 μm

wackestone matrix. The matrix, pellets, recrystallized shells and vein cements consist of low-Mg-calcite. Recrystallized shells are preferentially formed of a medium-grained granular cement but also contain clotted and laminated micritic crusts. These micritic crusts commonly bear rhomb-shaped crystals of a brown, inclusion-rich calcite, indicating that the primary mineralogy of these micrites was dolomitic. Pyrite is extremely rare. The petrography of the tube-worm limestone is similar to the *Lucina* limestone.

Botryoidal aragonite. One block found of botryoidal aragonite is composed almost entirely of botryoidal aragonite. The botryoids have a radius of up to 3.5 cm. They are only partly calcitized and are predominately preserved in their primary aragonitic mineralogy. Calcitization is directed from the periphery to the centre. Fibrous aragonite crystals originate from a dark-brown nuclear mass exhibiting no fluorescence (Fig. 9). Occasionally, the growth of crystals was interrupted and the fibres were covered by a concentric layer of dark-brown material, similar to the nuclear masses (Fig. 10a), but showing an intense fluorescence (Fig. 10b). Emerging from these layers the growth of a next generation of aragonite fibres continues.

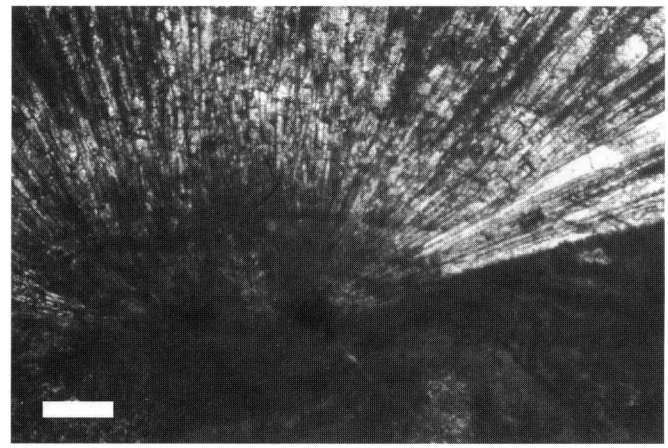

Fig. 9 The central portion of a botryoidal aragonite with aragonite fibres originating from a dark-brown nuclear mass, Marmorito. The *scale bar* corresponds to 500 μm

Marmorito limestone. All Marmorito limestones analysed in this study revealed a dolomitic composition of the matrix. Due to an intense in situ brecciation, calcitic fracture fillings crosscut the micro-crystalline dolomite. The surfaces of the sediment clasts are overgrown by coatings with a cloudy appearance. The thickness of the overgrowth varies from 10 to 1000 μm. They are also formed of dolomite and exhibit a globular fabric. Occasionally, the overgrowths form filamentous structures (Fig. 11a) which are then surrounded by the calcitic cements. The organic-rich overgrowth and especially the surfaces of the filamenteous structures exhibit an intense white (BP 365) or yellow (BP 450–490) fluorescence (Fig. 11b). Most intense fluorescence halos are observed as particular globules (Fig. 11c, d). Occasionally, some remains of these coatings are completely enclosed in the micro-crystalline dolomite (Fig. 11e, f), indicating that these organic-rich residues were enclosed during ongoing aggregation.

The FE–SEM analyses show that the overgrowths consist of three types of precipitate habits, which are crusts composed of hemispheres, rod-shaped crystal aggregates with rounded, brush-like terminations, and dumbbells (Fig. 12).

Stable isotopes and organic geochemistry

Beauvoisin

The $\delta^{13}C$ values of Lower Oxfordian carbonates vary widely between –26.5 and +13.0‰ PDB (Fig. 13). The

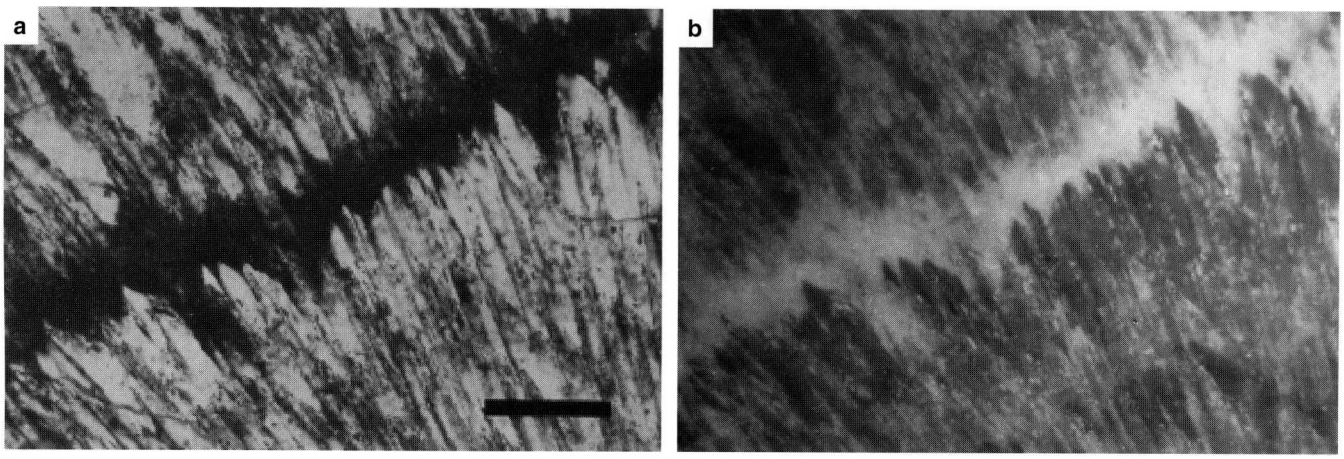

Fig. 10a,b Botryoidal aragonite, Marmorito. **a** Detail from a botryoidal aragonite with a concentric layer of dark-brown material, Marmorito. The *scale bar* corresponds to 250 μm. **b** Same section as **a**. The concentric layer shows an intense fluorescence, epifluorescence micrograph

nodules related to sponge taphonomy exhibit the most negative values (–26.5 to –22.8‰), whereas the direct adjacent internodular micrites range from –24.0 to +13.0‰. $\delta^{18}O$ values of early diagenetic carbonates range from –0.5 to +2.9‰ PDB. The stable isotope values of botryoidal aragonite exhibit a depletion in ^{13}C (–14.8 to –12.0‰) and in ^{18}O (–7.1 to –6.6‰). Carbonate concretions embedded in the marlstones distant from the pseudobioherms yielded $\delta^{13}C$ values of –19.0 and –17.7‰ and show a marine signature for oxygen ($\delta^{18}O$: –0.7 and +0.4‰ PDB). The marlstones surrounding both cold seep carbonates and carbonate concretions are enriched in ^{13}C (+0.8 and +1.1‰) and slightly depleted in ^{18}O (–1.3 and –0.8‰).

Variations in stable isotope values are less extreme in Middle and Upper Oxfordian carbonates, but still significant. A previous study revealed $\delta^{13}C$-values ranging from –13.6 to +15.1‰ and $\delta^{18}O$ values ranging from –1.2 to +0.7‰ (Gaillard et al. 1992). The Middle Oxfordian carbonates analysed in this study yielded $\delta^{13}C$ values that range from –13.7 to –10.1‰ and $\delta^{18}O$ values that range from –0.1 to +0.2‰.

Gas chromatograms ($C_{15}+$) of the total hydrocarbon fractions obtained from two Beauvoisin samples (Lower Oxfordian, Middle Oxfordian) are shown in Fig. 14. In both samples the main components are *n*-alkanes with chain lengths from 12 to 33 carbon atoms and a broad concentration maximum around *n*-heptadecane (*n*-C_{17}). With increasing chain lengths, *n*-alkane concentrations rapidly decrease. The observed, modal patterns are ubiquitously found in ancient sediments and crude oils. In fossil materials, they are of limited biomarker significance, since they may be generated from the thermal maturation of sedimentary organic matter rather than from a particular biological source input. A more distinctive feature of the Middle Oxfordian carbonates is the occurrence of several acyclic isoprenoid hydrocarbons ranging up to C_{35}. Two prominent members were identified as 2,6,10,15,19-pentamethylicosane (PME); according to IUPAC nomenclature, a C_{20} alkane is called icosane; hence, "PMI" would be the correct acronym]. However, the compound has commonly been referred to as 2,6,10,15,19-pentamethyleicosane (PME) heretofore. For reasons of compatibility, we also use this abbreviation.], and a C_{30} homologue 2,6,10,15,19,23-hexamethyltetracosane (squalane). In biogeochemistry and oil exploration geochemistry, PME and other acyclic isoprenoids with carbon skeletons in the range of C_{20} to C_{40} belong to the most widely used class of biomarkers for archaea, in particular methanogens (Brassell et al. 1981; Hahn 1982; Volkman et al. 1986; Wakeham 1990). The prominent abundance of PME thus reveals an indication for a pronounced activity of metharchaea associated with the formation of the Upper Oxfordian carbonates. The isotopic signatures of PME as well as squalane differ sharply from those observed for the *n*-alkane series. The latter show isotopic compositions normally found for marine lipids and petroleum hydrocarbons (around $\delta^{13}C$=-30‰ PDB), whereas both isoprenoids are significantly depleted in ^{13}C ($\delta^{13}C$=–75.7 and –67.5‰). The isotopic signatures of the *n*-alkanes indicate that they are not essentially autochthonous compounds, but at least partly originate from external, e.g. planktonic or detrital, sources. Even likely they represent petroleum constituents derived from ancient seepage fluids. On the other hand, our data suggest that the biosynthesis of the isoprenoids occured *in situ* and involved the utilization of isotopically depleted, seepage-derived carbon.

Marmorito

The $\delta^{13}C$ values of the investigated Marmorito limestone range from –40.2 to –17.3‰ (Fig. 13). The microcrystalline matrix (–40.2 to –38.9‰) yielded lower $\delta^{13}C$ values than the vein-filling calcitic cement (–28.5 to –17.3‰). The $\delta^{18}O$ values range from +4.8 to +4.9‰

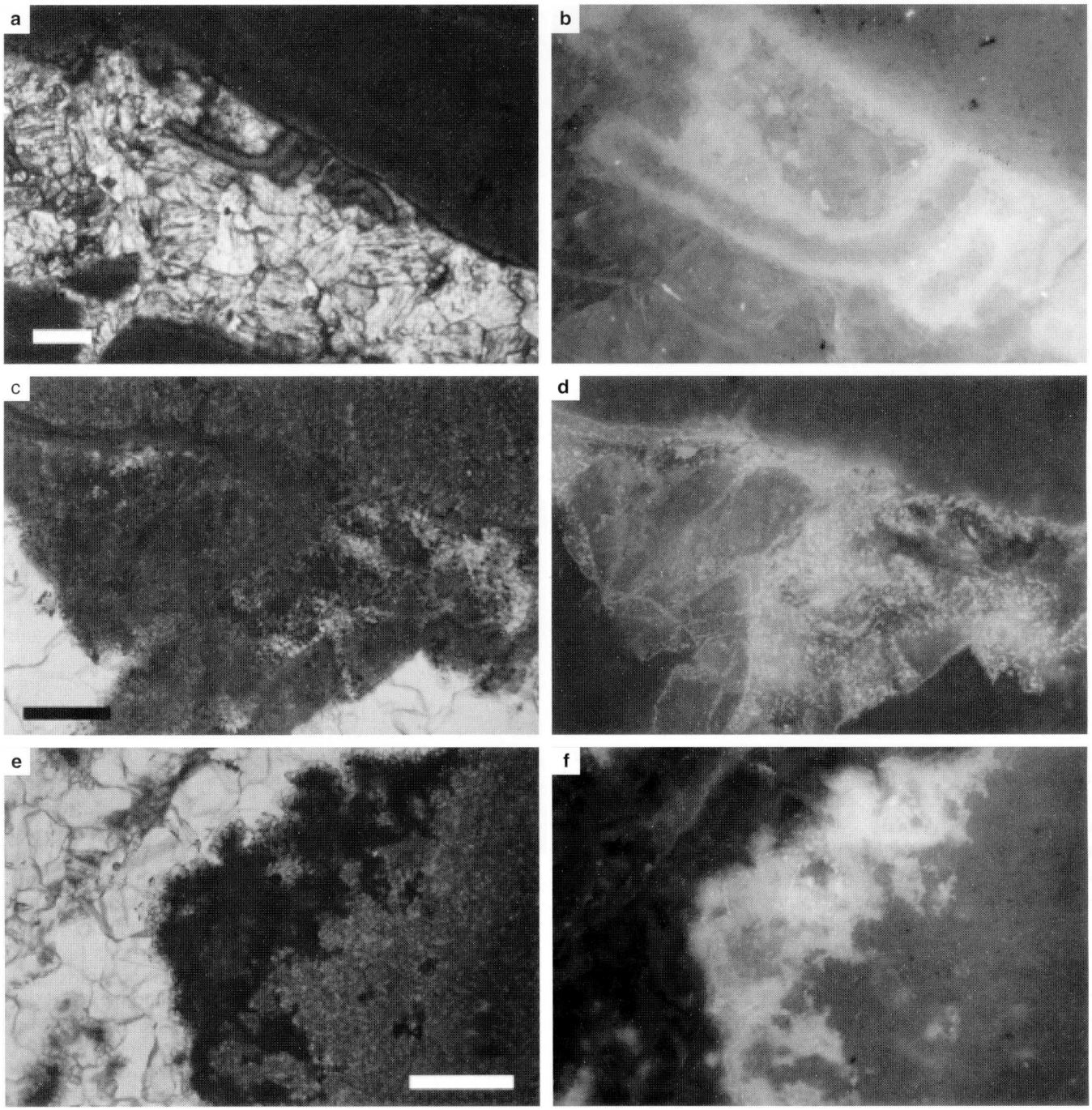

Fig. 11a–f Organic-rich remains within Marmorito carbonates. **a** Micro-crystalline dolomite (*dark*) crosscut by calcitic fracture fillings. Note the filamentous structures originating on the dolomite clast. Marmorito limestone. The *scale bar* corresponds to 500 μm. **b** Detail from **a**. The surfaces of the filaments exhibit an intense fluorescence, epifluorescence micrograph. **c** Matrix dolomite (*dark*) overgrown by a cloudy coating adjacent to the calcitic spar (*bright*). Marmorito limestone. The *scale bar* corresponds to 200 μm. **d** Same section as **c**. Most intense fluorescence halos are particular globules. **e** Calcitic spar (*left*), dolomitic coating and dolomitic matrix (*right*). Marmorito limestone. The *scale bar* corresponds to 250 μm. **f** Same section as **e**. The coating emits an intense fluorescence. Some remains of the phase that coats the dolomite clast are embedded in the matrix

in the dolomitic matrix and from +1.4 to +2.1‰ in the cements. The micrite of the tube-worm limestone is significantly ^{13}C depleted ($\delta^{13}C$: –32.9 to –26.6‰; $\delta^{18}O$: –0.4 to +0.1‰). The botryoidal aragonite exhibits $\delta^{13}C$ values ranging from –34.8 to –27.0‰ and a $\delta^{18}O$ values ranging from +0.3 to +2.7‰.

Biomarker analyses were performed on the Marmorito limestone and on the tube-worm limestone. A gas chromatogram of the total hydrocarbon fraction obtained from the tube-worm limestone is shown in Fig. 15. The main compound is PME, accompanied by its C_{20} homologue crocetane, an unusual compound which has only once been previously reported from

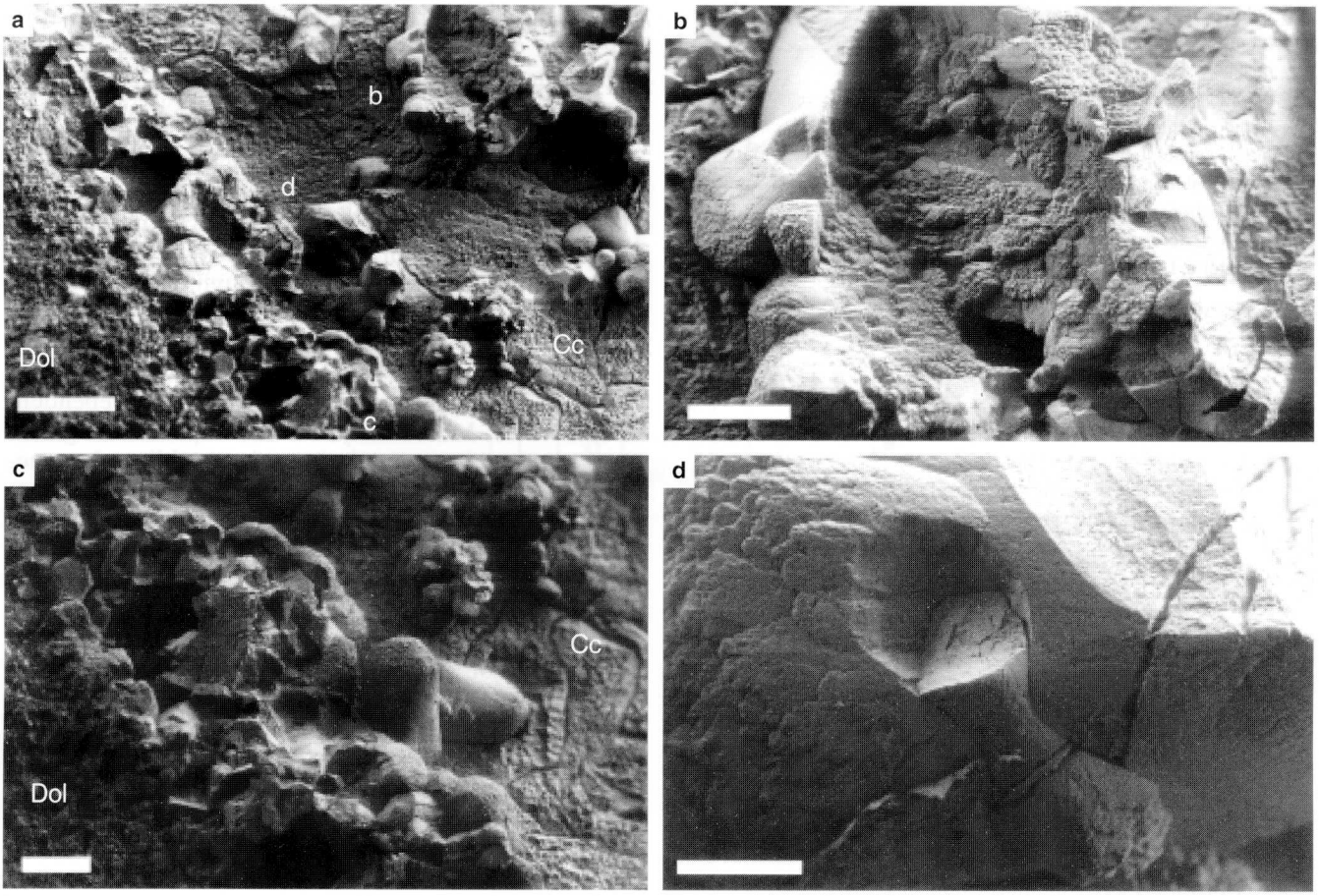

Fig. 12a–d FE–SEM images (EHT 0.8 kV) of the overgrowths on the clasts of the in situ brecciated Marmorito limestone. **a** The dolomitic micro-crystalline matrix (*Dol*), rod-shaped crystal aggregates of the overgrowth, and the calcitic cement (*Cc*). The letters *b, c,* and *d* mark the details shown in **b–d**. The *scale bar* corresponds to 100 μm. **b** Crusts composed of hemispheres. The *scale bar* corresponds to 30 μm. **c** Rod-shaped crystal aggregates (*centre*) between the dolomitic matrix (*Dol*) and the etched calcitic cement (*Cc*). The *scale bar* corresponds to 20 μm. **d** Centre of a rod-shaped crystal aggregate that contains a dumbbell-shaped crystal aggregate. The upper portion of the dumbbell is broken apart. The *scale bar* corresponds to 10 μm

ancient samples (McCarthy 1967; see Thiel et al. 1999 for further details). Both compounds are extremely depleted in ^{13}C. Their $\delta^{13}C$ values of –112 and –115‰ differ by approximately 80‰ from those of the normal alkanes present in the same sample. These features parallel the observations from the Middle Oxfordian Beauvoisin sample in an intriguing manner. They support the suggestion that certain archaea played a significant role in the biogeochemical cycling of carbon at these sites.

A different situation exists for the Marmorito limestone which shows only minor amounts of isoprenoid hydrocarbons. Instead, sterols and hopanols carrying an extra methyl group at C-4 and C-3, respectively, provide significant molecular markers in the alcohol fraction (Fig. 16). These compounds are not commonly observed among sedimentary lipids. Likely biological precursors were identified in recent methanotrophic bacteria, e.g. *Methylococcus capsulatus*, which produces 3-methylhopanepolyols (Neunlist and Rohmer 1985; Summons et al. 1994) as well as "primitive" sterols showing single or double methylation at C-4 (Bouvier et al. 1976). The presence of these or related compounds in the Marmorito limestone indicates a depositional environment, which at least temporarily permitted the growth of aerobic methanotrophs.

Discussion

Ancient chemosynthesis

Lucinid bivalves are the most prominent biota associated with the Oxfordian and Miocene cold seep carbonates. It has been presumed that they depended on chemosynthesis like their counterparts from the modern sea floor (Gaillard et al. 1992; Clari et al. 1994).

Sponges have been reported from some ancient seep deposits (Goedert and Squires 1990; Rigby and Goedert 1996). The "sponge nodules" of Beauvoisin which exhibit a clotted, bacterioform fabric and contain

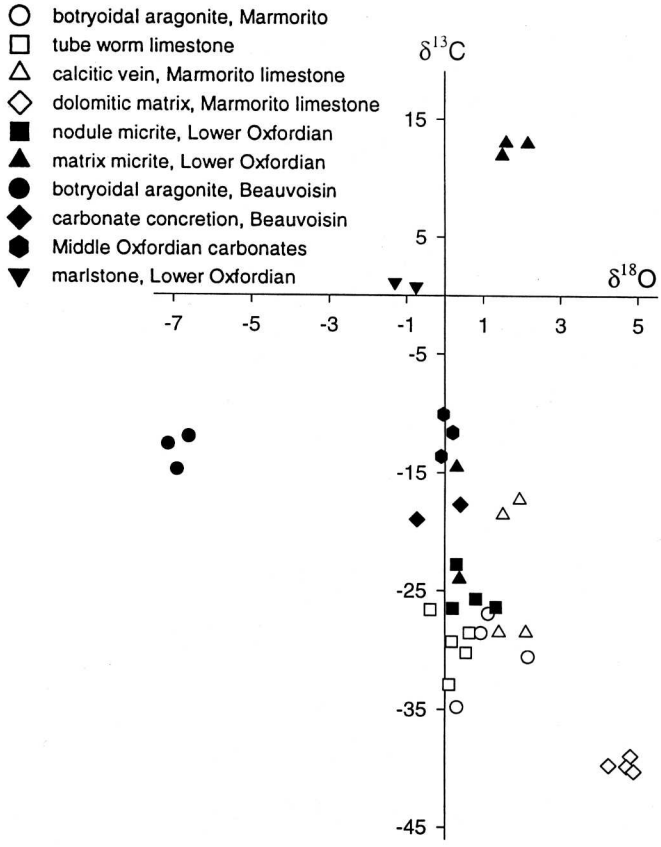

Fig. 13 Plot of the isotopic values of the carbonate phases from Beauvoisin and Marmorito analysed in this study. *Open symbols* Marmorito; *filled symbols* Beauvoisin

frequent spicules are considered to be a product of bacterial soft-tissue degradation. In particular, the activity of sulphate-reducing bacteria is indicated by the dispersely distributed framboidal pyrite within the nodules and by an outer rim of pyrite on the nodules. The enrichment of ^{12}C in the sponge nodules compared with the surrounding sediments may indicate that living sponges might have been linked to an enhanced hydrocarbon oxidation. Vacelet and Boury-Esnault (1995) reported on sponge-associated bacteria from cold methane seeps off Barbados, which display the morphological characteristics of methanotrophs. An uptake of carbon derived from microbial oxidation of hydrocarbons should result in ^{13}C depletion of the sponge biomass. Accordingly, the low $^{13}C_{carbonate}$ values of the sponge-nodules may result from the incorporation of CO_2 derived from bacterial sponge tissue degradation.

Most ancient seep carbonates contain remains of bivalves, but fossilized tube worms are rarely documented. Tube worms were recognized from another locality in the Miocene-age "calcari a *Lucina*" (Terzi et al. 1994). The authors report on "unidentified vestimentiferan-like tubular fossils". The tubes sampled during this study are too small in diameter to be attributed to vestimentifera, but resemble the smaller pogonophora in dimensions and shape. Pogonophora from modern cold seeps depend on methane as they harbour methanotrophic bacteria, which supply their hosts with nutrients and energy (Southward et al. 1981; Schmaljohann and Flügel 1987). The tube worms of Marmorito are embedded in a micritic carbonate that exhibits $\delta^{13}C$ values of approximately –30‰, thus indicating the seepage of methane through the sedimentary environment of the tube-worm colony. The presence of archaea-derived biomarkers in the tube worm limestone does not prove a contemporaneous coexistence of these micro-organisms with the oxygen-dependent invertebrates. More likely, these compounds originate from a subsurface population of the obligately anaerobic archaea, consistent with the view that methane-derived carbonates preferentially precipitate within the sediment (cf. Ritger et al. 1987; Gaillard et al. 1992).

Organic residues and their implications on the composition of the seepage fluids

Teichmüller and Ottenjann (1977) noticed that epifluorescence microscopy is a useful tool for detecting the relative distribution of organic residues enclosed in sedimentary rocks. In the hydrocarbon fractions of the Beauvoisin seep carbonates *n*-alkanes predominate. A connection between the content in aliphatic structures and the intense fluorescence of these rocks has to be taken into account. Bertrand et al. (1985) reported that fluorescence is favoured when chromophores (aromatic organic matter) are relatively isolated from each other within a dominantly aliphatic matrix. High concentrations of aromatic organic matter may result in interactions that inhibit fluorescence. This is due to an effect termed "concentration quenching" when chromophores absorb both the exciting and emitted wavelengths. In coal petrology it is well known that liptinites, which contain relatively large amounts of aliphatic constituents, exhibit the most intense fluorescence (Stach et al. 1982; Tissot and Welte 1984).

In the Oxfordian seep carbonates most intense fluorescence is observed on the edges of micro-cavities and veins where penetrating fluids might have been trapped. The *n*-alkanes enclosed in the Oxfordian carbonates were generated from thermal maturation of sedimentary organic matter. However, it is not evident whether the organic compounds were trapped after carbonate formation or seeped out of the sea floor syndepositionally. Notably, the carbon stable isotope composition of the Beauvoisin carbonates resembles that of carbonates from modern petroleum seeps (cf. Roberts and Aharon 1994).

Methane was a major component of the fluids of the Miocene Marmorito seep. This is revealed by $\delta^{13}C_{carbonate}$ values as low as –40‰ and chemofossils of methanotrophic bacteria.

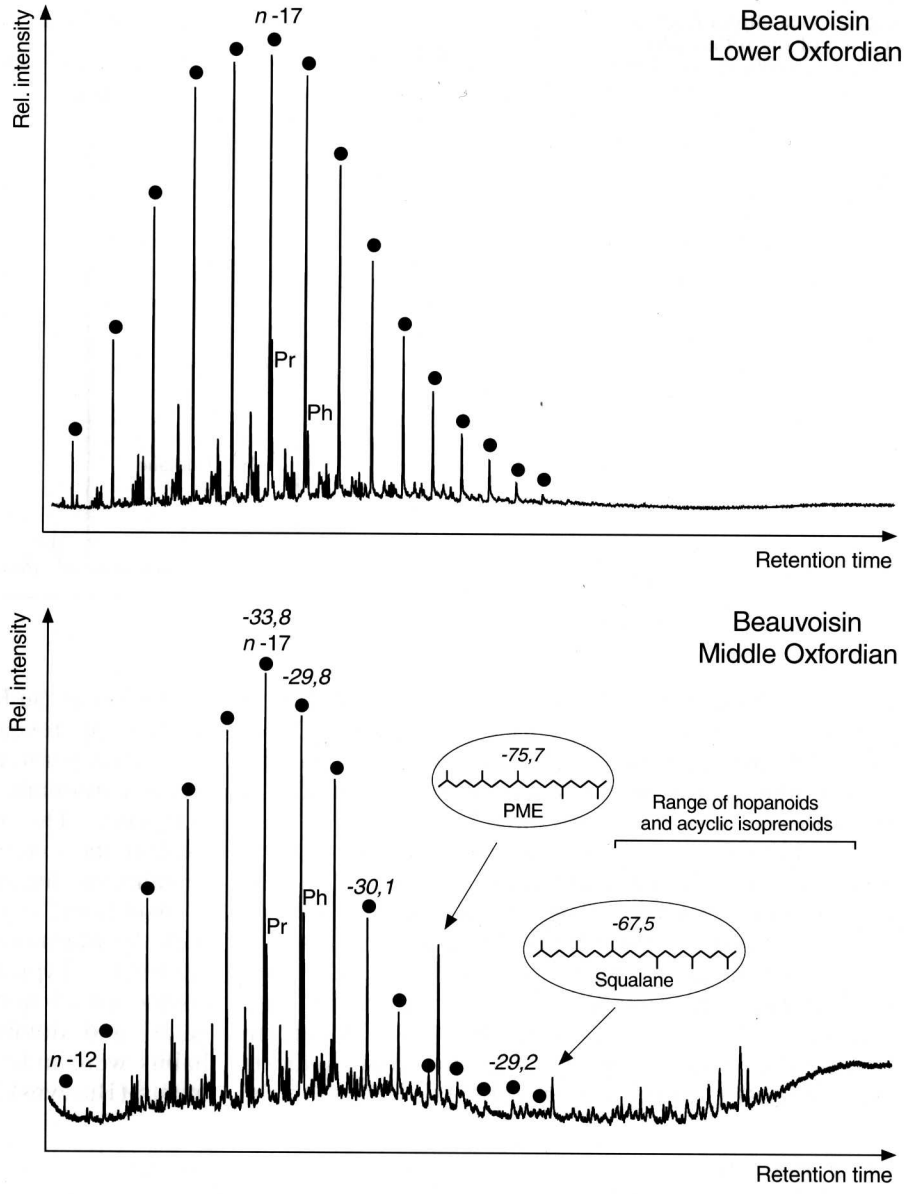

Fig. 14 Gas chromatogram ($C_{15}+$) of the hydrocarbon fractions obtained from the Upper Jurassic samples. *Numbers in italics* denote $\delta^{13}C$ values (vs PDB) measured by GC-C-IRMS. *Dots* *n*-alkanes, *n*-12 = *n*-dodecane, *n*-17 = *n*-heptadecane. PME = 2,6,10,15,19-pentamethylicosane; *Pr* pristane; *Ph* phytane. PME and squalane are regarded as biomarkers for methanogenic archaea

Microbial activity and carbonate precipitation

The Middle Oxfordian pseudobioherms contain biomarkers of archaea indicating a pronounced activity of methanogens associated with the carbonate formation. Methanogens were found to produce heavy CO_2 ($\delta^{13}C$: +24‰) resulting in ^{13}C-enriched carbonates precipitated in the methanic zone (Boehme et al. 1996). Indeed, Oxfordian carbonates exhibit $\delta^{13}C$ values as high as +15.1‰. In contrast, those Middle Oxfordian carbonates which contained the markers of archaea yielded $\delta^{13}C$ values that range from –13.7 to –10.1‰, thus indicating hydrocarbon oxidation rather than methane formation. The wide range in the carbon isotopic composition of the Lower Oxfordian carbonates implies that both methane formation and methane or hydrocarbon oxidation occurred in the same deposits and influenced carbonate formation. The low $\delta^{13}C$ values found for archaea-derived biomarkers from Marmorito may be assigned to anaerobic methane oxidation performed by a microbial consortium in which distinctive archaea participated (Thiel et al., in press; cf. Hinrichs et al. 1999). However, it should be stressed that a severe ^{13}C depletion may also result from fractionation effects during uptake of other substrates such as acetate or methylamine (e.g. Summons et al. 1998). The conclusion of a direct introduction of hydrocarbon carbon into cellular biomass by methanogenic archaea should thus be drawn with caution. Marmorito may thus be considered as an ancient counterpart of a known phenomenon which has frequently been reported from Recent sediments (Zehnder and Brock 1980; Hoehler et al. 1994; Harder 1997). In recent sediments anaerobic methane oxidation typically occurs at the base of the sulphate reduction zone and is ascribed to a consortium of sulphate

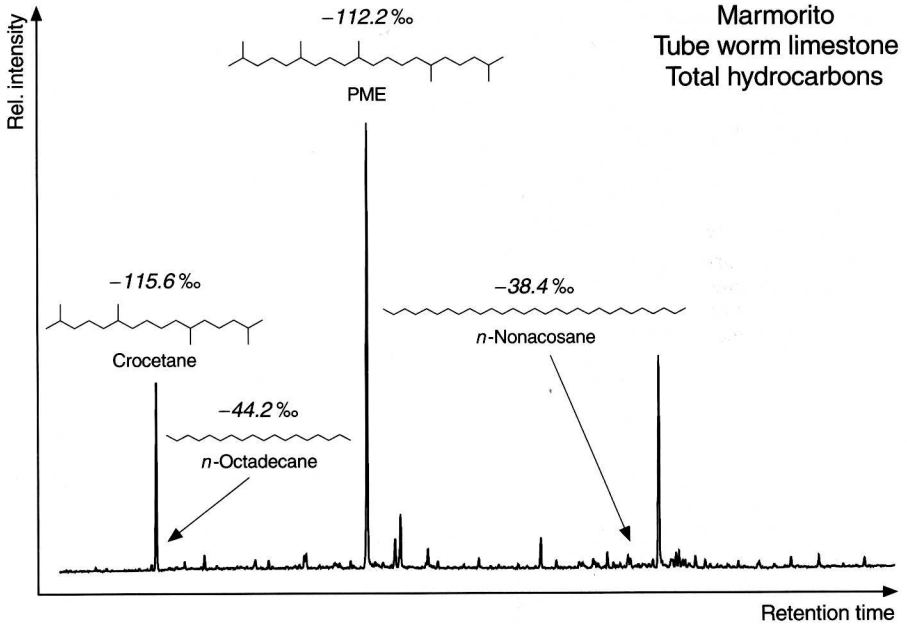

Fig. 15 Gas chromatogram ($C_{15}+$) of the total hydrocarbon fraction obtained from the Marmorito tube-worm limestone. *Numbers in italics* denote $\delta^{13}C$ values (vs PDB) measured by GC-C-IRMS. PME = 2,6,10,15,19-pentamethylicosane. PME and crocetane are regarded as biomarkers for archaea

reducers and archaea. Thus, we consider archaea to account not only for the ^{13}C enrichment in some phases of the Oxfordian carbonates, but also for the ^{13}C depletion in other phases of the Oxfordian carbonates and in the Miocene tube-worm limestone.

In addition to archaea, methanotropic bacteria are linked to the carbonate formation at cold seeps. The former presence of these organisms is crucial for the low $\delta^{13}C$ values of the Marmorito limestone (–40‰), since chemofossils of methanotrophs are most prominent in the sample studied. The biomarker data are corroborated by microscopic analyses. Abundant organic-rich overgrowths on dolomitic clasts indicate that bacterial biofilms were closely associated with the formation of the Marmorito limestone. Epifluorescence microscopy revealed that residues of these biofilms were incorporated into the micro-crystalline dolomite while carbonate aggregation extended towards the periphery. The resulting "in situ lithification" may explain the extraordinary preservation of the organic remains produced by these particular bacteria.

Additional evidence of bacterial activity associated with the Marmorito limestone is given by the FE-SEM analyses. Typical features observed are crusts composed of hemispheres, rod-shaped crystal aggregates, and dumbbells. Intriguingly, these precipitate habits were induced by bacteria in laboratory experiments (Buczynski and Chafetz 1991). Dolomite sphe-

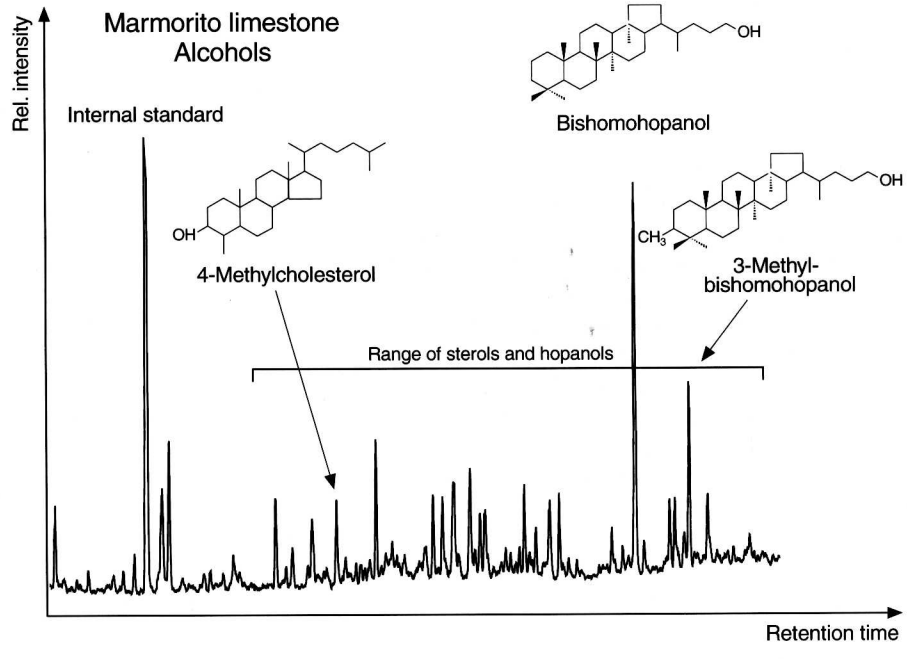

Fig. 16 Partial gas chromatogram of the alcohol fraction obtained from the Marmorito limestone (acetate derivatives). 4-Methylcholesterol and 3-methyl-bishomohopanol are regarded as biomarkers for aerobic methanotrophs

roids with dumbbell-shaped cores have previously been reported from the Marmorito limestone by Cavagna et al. (in press).

Micro-crystalline carbonates and botryoidal aragonite

Cold seep carbonates apparently show an excellent preservation potential with respect to metastable mineral phases and organic compounds. Examples for such metastable mineral phases are Mg-calcite from Beauvoisin or the botryoidal aragonites from both localities studied.

A high preservation potential may arise from the rapid calcification, and the protective sealing by less permeable pelagic or hemipelagic sediments such as claystones or marlstones. Savard et al. (1996) suggest that the preservation of aragonite within Cretaceous seep deposits is related to the engulfment of small acicular aragonite bundles in stable calcite. To the best of our knowledge, the Beauvoisin samples represent the oldest known seep carbonates which contain botryoids preserved in their primary mineralogy. However, the time of aragonite precipitation is yet unclear, as the botryoids (a) originate on iron-rich calcite, (b) are not overgrown by later phases and (c) exhibit $\delta^{18}O$ values of –7‰, in contrast to the less depleted early diagenetic carbonates (+2.8 to –0.5‰).

Roberts et al. (1993) reported that botryoidal aragonites from the Gulf of Mexico arise from nuclear masses of dark-brown substances and suggested that this material represents the remains of bacteria clumps. The Marmorito botryoids exhibit similar nuclear masses. The concentric layers within the botryoids are formed of similar matter and exhibit an intense fluorescence indicating an organic-rich composition. Organic nuclei like these supposed bacterial clumps may be able to trigger botryoidal aragonite formation. However, it is unlikely that they are essential for this process because not all botryoids from cold seeps display these features. It is also stressed that botryoidal aragonite is not confined to seep environments but is found in a variety of environments, e.g. reefs (James and Ginsburg 1979); therefore, methane-related bacterial activity is not crucial for its genesis.

It has been presumed that dolomite precipitation may occur at methane seeps due to the depletion of sulphate by bacterial sulphate reduction coupled with methane oxidation (Ritger et al. 1987). Sulphate is known as a very effective inhibitor of dolomite crystallization (Baker and Kastner 1981). The sample of the micro-crystalline Marmorito limestone exhibits no indication of dolomitization within the parts that are now formed of dolomite. The transition between dolomite and calcitic veins is always sharp and the phase boundary between the different mineralogies generally coincides with sedimentary fabrics. These properties may be interpreted in terms of a primary precipitation of dolomite at the ancient seep.

The $\delta^{18}O$ values of the dolomitic Marmorito limestone of approximately +5‰ have to be decreased by 3–4‰ because of the different oxygen isotope fractionation during crystallization of calcite and dolomite (O'Neil and Epstein 1966; Fritz and Smith 1970; Tan and Hudson 1971; Land 1980). After this subtraction all $\delta^{18}O$ values of the early diagenetic carbonate phases from Beauvoisin and Marmorito are close to 0‰, thus indicating a carbonate precipitated from waters of fairly low temperature. This implies a classification of the ancient settings as "cold seep" rather than "hot vent" environments.

Conclusion

The following conclusions were reached as a result of this study:

1. The relation of the Oxfordian carbonates from Beauvoisin and the Miocene carbonates from Marmorito to hydrocarbon seepage was confirmed.
2. Distinctive molecular signatures of archaea were observed in both Oxfordian and Miocene seep carbonates. Stable carbon isotope and biomarker analyses elucidate that both, archaeal methanogenesis and archaeal anaerobic methane oxidation, influenced the sedimentary environment and triggered carbonate precipitation.
3. Methanotrophic bacteria (aerobic methanotrophs) played a crucial role in the formation of the micro-crystalline Marmorito limestone. Extremely negative $\delta^{13}C$ values (–40‰) and the presence of particular biomarkers corroborate the importance of methanotrophs for carbon cycling. Organic-rich overgrowths on the resultant limestone clasts are formed of bacterial-induced precipiates and are interpreted as former biofilms and sites of carbonate aggregation.
4. In addition to lucinid bivalves, newly reported sponges (Beauvoisin) and tube worms resembling pogonophorans (Marmorito) are interpreted as ancient chemosynthetic taxa.
5. The Miocene seepage fluids (Marmorito) were dominated by methane. Oxfordian seepage fluids (Beauvoisin) were probably influenced by petroleum constituents, as indicated by the $C_{carbonate}$ isotopic composition and the hydrocarbon pattern.
6. Specific carbonate phases from the ancient cold seep deposits are micro-crystalline high-Mg-calcite (Beauvoisin), dolomite (Marmorito) and botryoidal aragonite (both sites).

Acknowledgements P. Albrecht, J. Hoefs, K. Simon and P. Wehrung are acknowledged for stable isotope measurements. We thank H. Becker and F. Brun for the preparation of thin sections and M. Hundertmark for photos of polished slabs. Our study was supported by the "Deutsche Forschungsgemeinschaft" (Mi-157/10–5,6; Th-713/1). This paper is a contribution to SFB 468 "Wechselwirkungen an geologischen Grenzflächen" (publication no. 14) at the University of Göttingen. We are grateful for the comments provided by G. Bohrmann (Kiel) and W. Oschmann (Frankfurt).

References

Baker P, Kastner M (1981) Constraints on the formation of sedimentary dolomite. Science 213:214–216

Beauchamp B, Savard M (1992) Cretaceous chemosynthetic carbonate mounds in the Canadian Arctic. Palaios 7:434–450

Bertrand P, Pittion J-L, Bernaud C (1985) Fluorescence of sedimentary organic matter in relation to its chemical composition. Org Geochem 10:641–647

Boehme SE, Blair NE, Chanton JP, Martens CS (1996) A mass balance of ^{13}C and ^{12}C in an organic-rich methane-producing marine sediment. Geochim Cosmochim Acta 60:3835–3848

Bouvier P, Rohmer M, Benveniste P, Ourisson P (1976) 8(14)-steroids in the bacterium *Methylococcus capsulatus*. Biochem J 159:267–271

Brassell SC, Wardroper AMK, Thomson ID, Maxwell JR, Eglinton G (1981) Specific acyclic isoprenoids as biological markers of methanogenic bacteria in marine sediments. Nature 290:693–696

Brönnimann P (1955) Microfossils incertae sedis from the Upper Jurassic and Lower Cretaceous of Cuba. Micropaleontology 1:28–57

Brönnimann P (1972) Remarks on the classification of fossil Anomuran coprolites. Paläontol Zeitschrift 46:99–103

Buczynski C, Chafetz HS (1991) Habit of bacterially induced precipiates of calcium carbonate and the influence of medium viscosity on mineralogy. J Sediment Petrol 61:226–233

Callender WR, Staff GM, Powell EN, Macdonald IR (1990) Gulf of Mexico hydrocarbon seep communities V. Biofacies and shell orientation of autochthonous shell beds below storm wave base. Palaios 5:2–14

Campbell KA, Carson C, Bottjer DJ (1993) Fossil cold seep limestones and associated chemosynthetic macroinvertebrate faunas, Jurassic–Cretaceous Great Valley Group, California. In: Graham SA, Lowe DR (eds) Advances in the sedimentary geology of the Great Valley Group, Sacramento Valley, California. Society of Economic Paleontologists and Mineralogists, Pacific Section, Book 73, pp 37–50

Cavagna S, Clari P, Martire L (1999) The role of bacteria in the formation of cold seep carbonates: geological evidence from Monferrato (Tertiary, NW Italy). Sediment Geol (in press)

Choquette PW, Trusell FC (1978) A procedure for making the Titan-Yellow stain for Mg-calcite permanent. J Sediment Petrol 48:639–641

Clari P, Gagliardi C, Governa ME, Ricci B, Zuppi GM (1988) I calcari de Marmorito: Una testimonianza di processidiagenetici in presenza di metano. Boll Museo Regionale Sci Naurali Torino 6:197–216

Clari P, Fornara L, Ricci B, Zuppi GM (1994) Methane-derived carbonates and chemosymbiotic communities of Piedmont (Miocene, northern Italy): an update. Geo-Mar Lett 14:201–209

Craig H (1957) Isotopic standards for carbon and oxygen and correction factors for mass-spectrographic analysis of carbon dioxide. Geochim Cosmochim Acta 12:133–149

Feigl F (1958) Spot test in inorganic analysis. Fifth enlarged and revised English edn. Elsevier, Amsterdam, pp 1–600

Fritz P, Smith DGW (1970) The isotopic composition of secondary dolomites. Geochim Cosmochim Acta 34:1161–1173

Gaillard C, Bourseau JP, Boudeulle M, Pailleret P, Rio M, Roux M (1985) Les pseudobiohermes de Beauvoisin (Drôme): un site hydrothermal sur la marge téthysienne à l'Oxfordien ? Bull Soc Géol France 1:69–78

Gaillard C, Rolin Y (1988) Relation entre tectonique synsédimentaire et pseudobiohermes (Oxfordien de Beauvoisin-Drôme-France). Un argument supplémentaire pour interpréter les pseudobiohermes comme formés au droit de sources sous-marines. C R Acad Sci Paris 307:1265–1270

Gaillard C, Rio M, Rolin Y, Roux M (1992) Fossil chemosynthetic communities related to vents or seeps in sedimentary basins: the pseudobioherms of southeastern France compared to other world examples. Palaios 7:451–465

Goedert JL, Squires RL (1990) Eocene deep-sea communities in localized limestones formed by subduction-related methane seeps, southwestern Washington. Geology 18:1182–1185

Hahn J (1982) Geochemical fossils of a possibly archaebacterial origin in ancient sediments. Zbl Bakt Hyg, I Abt Orig C 3:40–52

Harder J (1997) Anaerobic methane oxidation by bacteria employing ^{14}C-methane uncontaminated ^{14}C-carbon monoxide. Mar Geol 137:13–23

Hashimoto J, Ohta S, Tanaka T, Hotta H, Matsuzawa H, Sakai H (1989) Deep-sea communities dominated by the giant clam *Calyptogena soyoae* along the slope foot of Hatsushima island, Sagami Bay, Central Japan. Palaeogeogr Palaeoclimatol Palaeoecol 71:179–192

Hinrichs K-U, Hayes JM, Sylva SP, Brewer PG, DeLong EF (1999) Methane-consuming archaebacteria in marine sediments. Nature 398:802–805

Hoehler T, Alperin MJ, Albert DB, Martens C (1994) Field and laboratory studies of methane oxidation in an anoxic marine sediment: evidence for a methanogen-sulfate reducer consortium. Global Biogeochem Cycles 8:451–463

Hovland M, Talbout M, Qvale H, Olausson S, Aasberg L (1987) Methane-related carbonate cements in pockmarks of the North Sea. J Sediment Petrol 57:881–892

James NP, Ginsburg RN (1979) The seaward margin of Belize Barrier and Atoll Reefs. IAS Spec Publ 3:1–191

Jannasch HW (1984) Chemosynthesis: the nutritional basis for life at deep-sea vents. Oceanus 27:73–78

Jörgensen NO (1989) Holocene methane-derived, dolomite cemented sandstone pillars from the Kattegat, Denmark. Mar Geol 88:71–81

Juniper SK, Sibuet M (1987) Cold seep benthic communities in Japan subduction zones: spatial organization, trophic strategies and evidence for temporal evolution. Mar Ecol Prog Ser 40:115–126

Kennicutt MC II, Brooks JM, Bidigare RR, Fay RR, Wade TL, MacDonald TJ (1985) Vent-type taxa in a hydrocarbon seep region on the Louisiana slope. Nature 317:351–353

Kim S-T, O'Neil JR (1997) Equilibrium and nonequilibrium oxygen isotope effects in synthetic carbonates. Geochim Cosmochim Acta: 3461–3475

Land LS (1980) The isotopic and trace element geochemistry of dolomite: the state of the art. In: Zenger DH, Dunham JB, Ethington RL (eds) Concepts and models of dolomitization. SEPM Spec Publ 28:87–110

McCarthy ED (1967) A treatise in organic geochemistry. PhD thesis, University of California

Neunlist S, Rohmer M (1985) Novel hopanoids from the methylotrophic bacteria *Methylococcus capsulatus* and *Methylomonas methanica*. Biochem J 231:635–639

O'Neil JR, Epstein S (1966) Oxygen isotope fractionation in the system dolomite-calcite-carbon dioxide. Science 152:198–201

Paull CK, Hecker B, Commeau R, Freeman-Lynde RP, Neumann C, Corso WP, Golubic S, Hook JE, Sikes E, Curray J (1984) Biological communities at the Florida Escarpment resemble hydrothermal vent taxa. Science 226:965–967

Ricci Lucchi F, Vai GB (1994) A stratigraphic and tectonofacies framework of the "calcari a Lucina" in the Apennine Chain, Italy. Geo-Mar Lett 14:210–218

Rigby JK, Goedert JL (1996) Fossil sponges from a localized cold-seep limestone in Oligocene rocks of the Olympic Peninsula, Washington. J Paleontol 70:900–908

Ritger S, Carson B, Suess E (1987) Methane-derived authigenic carbonates formed by subduction-induced pore-water expulsion along the Oregon/Washington margin. Geol Soc Am Bull 98:147–156

Roberts HH, Aharon P (1994) Hydrocarbon-derived carbonate buildups of the northern Gulf of Mexico continental slope: a review of submersible investigations. Geo-Mar Lett 14:135–148

Roberts HH, Aharon P, Walsh MM (1993) Cold-seep carbonates of the Louisiana continental slope-to-basin floor. In: Rezak R, Lavoie DL (eds) Carbonate microfabrics. Springer, Berlin Heidelberg New York, pp 95–104

Rolin Y, Gaillard C, Roux M (1990) Ecologie des pseudobiohermes des Terres Noires jurassiques liés à des paléo-sources sous-marines. Le site oxfordien de Beauvoisin (Drôme, bassin du Sud-Est, France). Palaeogeogr Palaeoclimatol Palaeoecol 80:79–105

Rosman I, Bolan GS, Baker JS (1987) Epifaunal aggregations of Vesicomyidae on the continental slope off Louisiana. Deep-Sea Res 34:1811–1820

Savard MM, Beauchamp B, Veizer J (1996) Significance of aragonite cements around cretaceous marine methane seeps. J Sediment Res 66:430–438

Schmaljohann R, Flügel HJ (1987) Methane-oxidizing bacteria in Pogonophora. Sarsia 72:91–98

Sharma T, Clayton RN (1965) Measurement of O^{18}/O^{16} ratios of total oxygen of carbonates. Geochim Cosmochim Acta 29:1347–1353

Sibuet M, Olu K (1998) Biogeography, biodiversity and fluid dependence of deep-sea cold-seep communities at active and passive margins. Deep-Sea Res II 45:517–567

Southward AJ, Southward EC, Dando PR, Rau GH, Felbeck H, Flügel H (1981) Bacterial symbionts and low $^{13}C/^{12}C$ ratios in tissues of Pogophora suggest unusual nutriation and metabolism. Nature 293:616–620

Stach E, Mackowsky MT, Teichmüller M, Taylor GH, Chandra D, Teichmüller R (1982) Stach's textbook of coal petrography. Borntraeger, Berlin

Suess E, Carson B, Ritger SD, Moore JC, Jones ML, Kulm LD, Cochrane GR (1985) Biological communities at vent sites along the subduction zone off Oregon. Biol Soc Wash Bull 6:475–484

Suess E, Whiticar MJ (1989) Methane-derived CO_2 in pore fluids expelled from the Oregon subduction zone. Palaeogeogr Palaeoclimatol Palaeoecol 71:119–136

Summons RE, Jahnke LL, Roksandic Z (1994) Carbon isotopic fractionation in lipids from methanotrophic bacteria: Relevance for interpretation of the geochemical record biomarkers. Geochim Cosmochim Acta 58:2853–2863

Summons RE, Franzmann PD, Nichols PD (1998) Carbon isotopic fractionation associated with methylotrophic methanogenesis. Org Geochem 28:465–475

Tan FC, Hudson JD (1971) Carbon and oxygen relationships of dolomites and co-existing calcites, Great Estuarine Series (Jurassic), Scotland. Geochim Cosmochim Acta 35:755–767

Teichmüller M, Ottenjann K (1977) Liptinite und lipoide Stoffe in einem Erdölmuttergestein. Erdöl Kohle 30:387–398

Terzi C, Aharon P, Ricci Lucchi F, Vai BG (1994) Petrography and stable isotope aspects of cold-vent activity imprinted on Miocene-age "calcari a *Lucina*" from Tuscan and Romagna Apennines, Italy. Geo-Mar Lett 14:177–184

Thiel V, Peckmann J, Seifert R, Wehrung P, Reitner J, Michaelis W (1999) Highly isotopically depleted isoprenoids: molecular markers for ancient methane venting. Geochim Cosmochim Acta (in press)

Tissot BP, Welte DH (1984) Petroleum formation and occurrence: a new approach to oil and gas exploration. Springer, Berlin Heidelberg New York

Vacelet J, Boury-Esnault N (1995) Carnivorous sponges. Nature 373:333–335

Volkman JK, Allen DI, Stevenson PL, Burton HR (1986) Bacterial and algal hydrocarbons from a saline Antarctic lake, Ace Lake. Org Geochem 10:671–681

Wakeham SG (1990) Algal and bacterial hydrocarbons in particulate matter and interfacial sediment of the Cariaco Trench. Geochim Cosmochim Acta 54:1325–1336

Whiticar MJ, Faber E, Schoell M (1986) Biogenic methane formation in marine and freshwater environments: CO_2 reduction vs acetate fermentation-isotope evidence. Geochim Cosmochim Acta 50:693–709

Zehnder AJB, Brock TD (1980) Anaerobic methane oxidation: occurrence and ecology. Appl Environ Microbiol 39:194–204